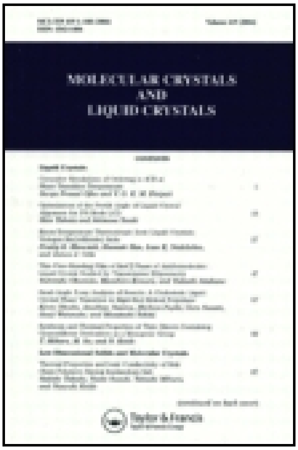

Molecular Crystals and Liquid Crystals Science and Technology. Section A. Molecular Crystals and Liquid Crystals

Publication details, including instructions for authors and subscription information:
http://www.tandfonline.com/loi/gmcl19

Mapping of Redox Energies

J. B. Goodenough [a]

[a] Center for Materials Science & Engineering, ETC 9.102 University of Texas at Austin, Austin, TX, 78712-1063

Version of record first published: 04 Oct 2006

Mol. Cryst. Liq. Cryst., 1998, Vol. 311, pp. 1-14
Reprints available directly from the publisher
Photocopying permitted by license only

MAPPING OF REDOX ENERGIES

J. B. Goodenough
Center for Materials Science & Engineering, ETC 9.102
University of Texas at Austin, Austin, TX 78712-1063

Electrochemical discharge/charge curves vs Lithium of coin cells using as cathodes various transition-metal oxide hosts for lithium insertion/extraction reactions provide information on the operative redox energies of the transition-metal atoms. The relative positions of the redox energies were found to vary little, but their absolute positions by as much as 1 eV, with changes in structure or, for an isostructural series, with changes in counter cation. Use of polyanions to obtain a more open framework with a larger free volume for Li^+-ion motion was found to be more important for high-power applications than the loss in electronic mobility, but a larger free volume for ionic motion reduces the capacity per unit volume. It was shown that introduction of a second phase with a higher redox energy provides a buffer against over discharge. A reversible decrease in capacity with increasing current density was identified and its origin discussed. Substitution of the polyanions $(PO_4)^{3-}$ or $(SO_4)^{2-}$ for oxide ions brings the V^{4+}/V^{3+} and Fe^{3+}/Fe^{2+} redox energies to levels of interest for cathodes in a lithium-ion battery.

Keywords: battery, lithium-ion; insertion compounds; polyanion structures.

INTRODUCTION

The redox energies of transition-metal cations in oxides vary with the structure of the oxide and any counter cation present. Location of these redox energies and control of their variations in different oxides are important for the design of lithium-ion batteries and heterogeneous catalysts; they are also relevant to our theoretical understanding of the electronic and magnetic properties of transition-metal oxides. Oxides that are hosts to the insertion of lithium as a guest species allow the use of electrochemistry to locate redox energies relative to the Fermi energy of a lithium anode.

The layered compounds Li_xMX_2, $0 \le x \le 1$ and X = O or S, offer two-dimensional (2D) pathways for lithium insertion, the spinels $Li_y[M_2]X_4$ offer 3D pathways, each in a close-packed anion array; the operative redox couple is M^{4+}/M^{3+} for all x or y. The performances of the layered TiS_2 and spinel $[Ti_2]S_4$ hosts, Fig. 1, are nearly identical [1]; in each case, lithium is inserted only into interstitial octahedral sites and the S^{2-} ions are large enough to provide sufficient free volume for a good Li^+-ion mobility even in the spinel host where strong 3D bonding constrains the free volume for Li^+-ion motion. In these compounds, the Li^+ ions occupy a set of crystallographically (hence energetically) equivalent sites, and the variation in the open-circuit voltage V_{oc} with site occupancy follows a Nernst law for the dependence of the chemical potential on lithium activity [2] despite the metallic character of the two systems.

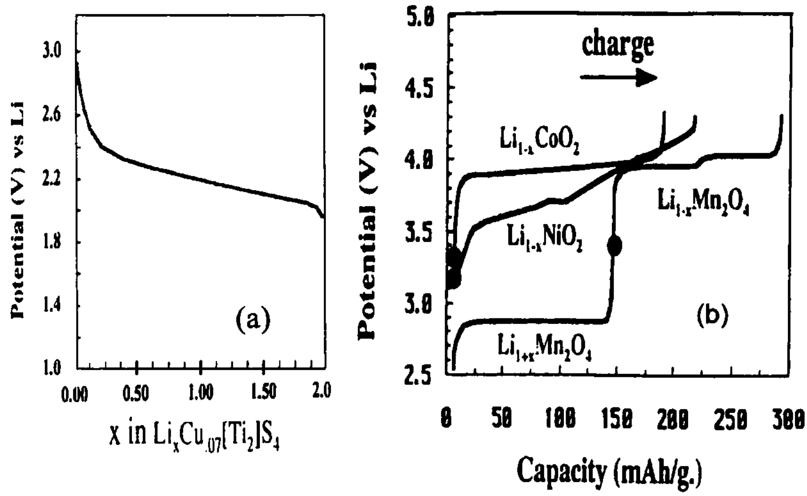

FIGURE 1 The open-circuit voltage vs lithium for
(a) $Li_xCu_{0.7}[Ti_2]S_4$, $0 \le x \le 2$, and (b) the layered oxides
(b) $Li_{1-x}CoO_2$, $Li_{1-x}NiO_2$ and the spinel $Li_{1\pm x}[Mn_2]O_4$.

Unlike the sulfides, the oxides permit access to the formal Co^{4+}/Co^{3+} and Ni^{4+}/Ni^{3+} redox energies, but the smaller size of the oxide ions limits the room-temperature mobility of the Li^+ ions in an $[M_2]O_4$ spinel framework relative to the 2D Li^+-ion mobility in the layered oxides having a degree of freedom to open up the Li^+-ion layers[3]. The Li^+ ions occupy tetrahedral sites in the system $Li_{1-x}[Mn_2]O_4$ [4]. As originally emphasized [5] in a study of $Li_{1+x}[Ti_2]O_4$, there is a remarkable change ÆV_{oc} Å 1.0 V in the open-circuit voltage that accompanies a transfer of the Li^+ ions from the tetrahedral to the octahedral sites [6]; it is a measure of the stabilization of the spinel *vs* the cation-deficient rock-salt structure in a parent $Li[Mn_2]O_4$ compound. Moreover, there is a change from 3.9 to 4.1 V at $x = 0.5$ in $Li_{1-x}[Mn_2]O_4$. This change appears to reflect a change in the Li^+-Li^+ interactions in the tetrahedral sites as Li^+ ions are removed preferentially from one of the two interpenetrating face-centered-cubic arrays that compose the 8a tetrahedral sites of the spinel structure. These changes in voltage with occupancy of the interstitial sites by Li^+ ions demonstrate an important dependence of the M^{4+}/M^{3+} redox energy on the structure and prompt exploration of how redox energies change not only with structure, but also with the counter cation in an isostructural series of compounds. Moreover, the fact that the V_{oc} of $Li[Mn_2]O_4$ lies midway between the plateau at 3 V and 4 V signals that cooperative, dynamic Jahn-Teller deformations associated with the Mn^{3+} ions may have induced a segregaton into Mn^{3+}-rich domains containing octahedral-site Li^+ ions and Mn^{3+}-poor domains containing tetrahedral-site Li^+ ions.

Fig. 2 illustrates the construction of the electron energies for MnO starting from an ionic model. E_I represents the energy required to remove an electron from a Mn^+ ion (second ionization energy) and place it on an O^- ion (negative electron affinity). Assembling the ions into the rock-salt structure returns the electrostatic Madelung energy E_M ; the internal electric field raises all the cation energies by $E_M/2$ and lowers the anion energies by $-E_M/2$, thereby conserving the total energy of the system. An ionic model requires an $E_M > E_I$. The O^{2-} - O^{2-} and Mn^{2+} - Mn^{2+} interactions broaden the O^{2-}:$2p^6$ and Mn^{2+}:$4s^0$ levels into valence and conduction bands, respectively. The covalent back transfer of electrons from the O^{2-} ions can be treated in second-order perturbation theory; the resultant lowering of E_M is largely compensated by the quantum-mechanical repulsion between bonding and antibonding states, which is why an ionic model gives a good estimate of the binding energy of the compound. However, care must be taken in partitioning the covalent compensation between different antibonding states. A larger O:2p-orbital overlap with the Mn 4s orbitals relative to the Mn 3d orbitals raises the center of the 4s band relative to the narrow Mn:$3d^5$ localized-electron level lying in the gap between conduction and valence bands. Of particular importance in compounds with two cations is the partitioning of covalent bonding between two different cations sharing the same bridging anion; stronger covalent bonding with one lowers the redox energy at the other. This inductive effect is stronger the larger the M-O-M' bridging angle.

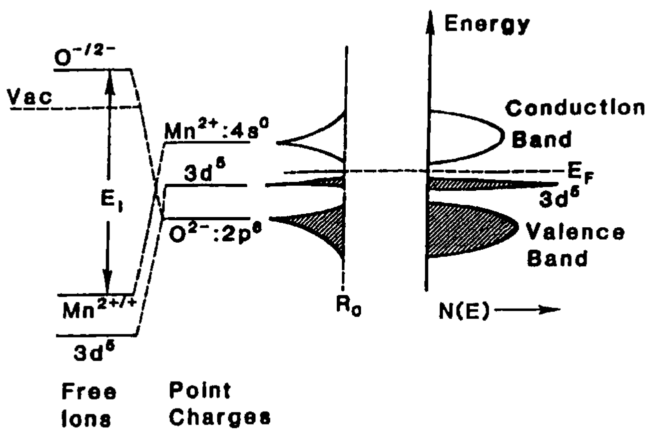

FIGURE 2 Schematic construction of electronic energies in MnO starting from an ionic model.

The redox energies in various oxide hosts relative to the Fermi energy of lithium have been obtained by measuring the voltages V of coin cells (type 2023) having a lithium-foil anode with a current density of 0.05

mA/cm^2 . At this low current density, the voltage approaches the open-circuit value (V Å V_{oc}). The electrolyte (Mitsubishi Chemical Co., Ltd.) was 1 M $LiClO_4$ in a 1:1 (by volume) mixture of propylene carbonate (PC) and dimethoxyethane (DME); it limited the voltage of the cells to V < 4.3 V.

The larger is the crystalline electric field and covalent bonding at the operative transition-metal ion M of the oxide host used as a cathode, the higher is the energy of the highest occupied antibonding redox energy and the lower is the measured V_{oc}. The point-charge crystalline electric field at the cation is determined by the structure; the influence of the counter cation can be monitored by measuring V_{oc} for a given redox energy in isostructural compounds containing different counter cations. Framework structures containing polyanions in place of oxide ions have been used to demonstrate the influence of the counter cation.

The cathode materials were ground to fine particles with a milling machine (Spex #8000 mixer/mill). The active fine particles were blended with acetylene black (Denki Kagaku Co., Ltd.) and polytetrafluorene (Polyflon TFE-103, Daikin Industry, Ltd.) in the weight ratio 75:25:5. This cathode mixture was rolled into thin sheets of uniform thickness and cut into pellets of the required size for coin-cell fabrication (2 cm^2, *ca.* 100 mg). Cell performance was evaluated at various constant currents (0.05-1 mA/cm^2) at room temperature with an Arbin Battery Tester System (ASTS).

II. RESULTS

1. **Spinels containing pentavalent vanadium.** The introduction of V^{5+} ions into the tetrahedral sites of the $V[Li_{1-x}M]O_4$ spinels allows probing of the energies of the M^{3+}/M^{2+} couples; however, these spinels are not useful as battery cathodes since the coexistence of M and Li on the octahedral sites limits the capacity and Li^+-ion mobility. Fey *et al* [7] obtained a voltage plateau of 4.2 and 4.8 V with a current density of 0.05 mA/cm^2 for the Co^{3+}/Co^{2+} and Ni^{3+}/Ni^{2+} couples, respectively, using $LiPF_6$ as the electrolyte salt. We [8] prepared the M =

Mn spinel under high pressure and obtained a plateau of 3.8 V for the Mn^{3+}/Mn^{2+} couple at the same current density. We were unable to prepare the M = Fe spinel; the tetrahedral-site V^{5+}/V^{4+} couple apparently has an energy between those of Fe^{3+}/Fe^{2+} and Mn^{3+}/Mn^{2+} couples, which would give Fe^{3+}/V^{4+} rather than Fe^{2+}/V^{5+} in the parent spinel. What is significant is that replacement of Li^+ by V^{5+} on the tetrahedral sites has polarized the charge on the O^{2-} ion toward the V^{5+} ions in a strongly covalent VO_4 complex, which lowers the redox energies of the octahedral-site M cations. Whereas the Mn^{4+}/Mn^{3+} couple was at 3.9 V *vs*. lithium in $Li_{1-x}[Mn_2]O_4$, it is the Mn^{3+}/Mn^{2+} couple that is at 3.8 V in $V[Li_{1-x}Mn]O_4$.

2. **Ordered olivines containing pentavalent phosphorus.** Substitution of $(PO_4)^{3-}$ for $(VO_4)^{3-}$ stabilizes the ordered olivines $Li_{1-x}MPO_4$ [9]. In the olivines, the oxygen atoms are nearly hexagonal-close-packed; and in the ordered olivine structure, the M cations occupy zig-zag chains in alternate octahedral-site (001) planes; these chains are bridged by corner- and edge-sharing $(PO_4)^{3-}$ polyanions to form a host structure with strong 3D bonding as in a spinel. The Li^+ ions occupy the remaining octahedral-site (001) planes, which makes 2D motion possible. However, the Li^+ions are ordered within these (001) planes along chains of edge-shared octahedra, which constrains the Li^+-ion motion to be preferentially along the orthorhombic *b*-axis. All the lithium can be removed chemically to give the framework host $FePO_4$ having the same space group, but extraction of lithium from $Li_{1-x}FePO_4$ or insertion of lithium into Li_yFePO_4 occurs via a two-phase plateau at 3.5 V for a current density of 0.05 mA/cm^2 with a capacity of only 0.6 Li per formula unit.

We were unable to extract Li from $LiMnPO_4$, but we could prime the extraction by substituting some Fe for Mn. Fig. 3 shows the V *vs* x curves at 0.05 mA/cm^2 for $LiMn_{0.5}Fe_{0.5}PO_4$; the Fe^{3+}/Fe^{2+} redox energy remains near 3.5 V *vs* lithium whereas the Mn^{3+}/Mn^{2+} couple gives a plateau at about 4.1 V. Apparently each transition-metal ion retains its own equilibrium M-O bond length, which holds the redox couples at characteristic energies for a given structure and counter cation. It is this behavior that makes possible identification and mapping of the redox energies in an isostructural series of compounds [10].

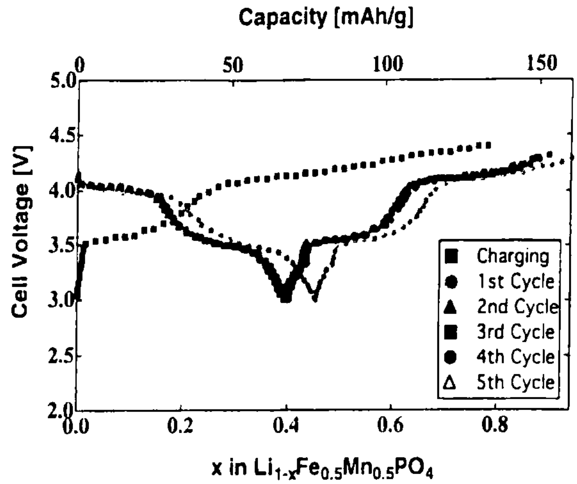

FIGURE 3 Cell voltage vs lithium for the ordered olivine $Li_{1-x}Fe_{0.5}Mn_{0.5}PO_4$.

3. **Comparing octahedral-site Fe^{3+}/Fe^{2+} redox energies.** The effect of structure on the Fe^{3+}/Fe^{2+} redox energy is demonstrated by comparing a V_{oc} Å 3.5 V in $LiFePO_4$ with a V_{oc} = 3.1 V and 2.9 V in the pyrophosphates $Li_xFe_4(P_2O_7)_3$ and $Li_{1+x}FeP_2O_7$ [11] and a V_{oc} = 2.8 V in $Li_{3+x}Fe_2PO_4$ with the rhombohedral NASICON structure of Fig.4[12]. In $LiFePO_4$, each FeO_6 octahedron shares an edge with a $(PO_4)^{3-}$ polyanion, which lowers the Madelung electric field at the Fe atoms relative to that in the NASICON structure where the FeO_6 octahedra share only corners with the bridging $(PO_4)^{3-}$ polyanions. The FeO_6 octahedra share only corners with the $(P_2O_7)^{4-}$ polyanions in the two pyrophosphates, but pairs of FeO_6 octahedra share common faces in $Li_xFe_4(P_2O_7)_3$,which lowers the Madelung electric field at the Fe atoms relative to that in $Li_xFeP_2O_7$.

The effect of the counter cation D on the Fe^{3+}/Fe^{2+} redox energy is demonstrated by the isostructural series of compounds having the rhombohedral NASICON structure with the $Fe_2(DO_4)_3$ host framework illustrated in Fig. 4.

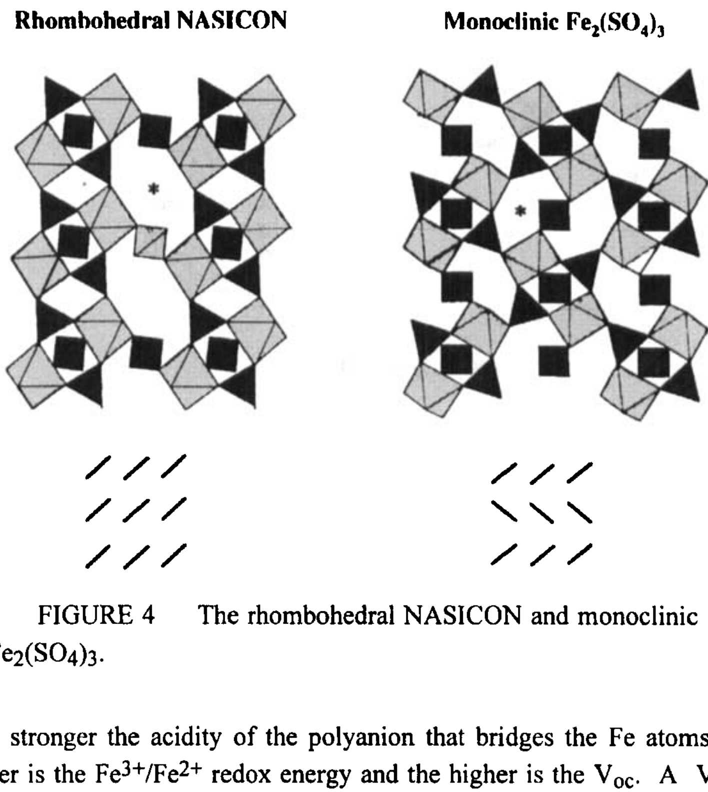

FIGURE 4 The rhombohedral NASICON and monoclinic forms of $Fe_2(SO_4)_3$.

The stronger the acidity of the polyanion that bridges the Fe atoms, the lower is the Fe^{3+}/Fe^{2+} redox energy and the higher is the V_{oc}. A V_{oc} = 3.6 V in $Li_xFe_2(SO_4)_3$ *vs* a V_{oc} = 3.0 V in $Li_xFe_2(MoO_4)_3$ and $Li_xFe_2(WO_4)_3$ were first recognized [13] to reflect this inductive effect. The V_{oc} = 2.8 V found [12] for $Li_{3+x}Fe_2(PO_4)_3$ represents a raising by 0.8 eV of the energy of the Fe^{3+}/Fe^{2+} redox couple on changing the $(SO_4)^{2-}$ polyanion to $(PO_4)^{3-}$; this shift was essentially the same for all redox energies investigated. The relative energies remained fixed, the absolute energies of each changed by about the same amount on passing from one structure to another and from one polyanion to another. However, the concentration and distribution of the Li^+ ions can be important, as was demonstrated in the spinel systems $Li_{1\pm x}[Mn_2]O_4$.

In order to investigate the influence of three additional Li atoms in the interstitial space of $Li_3Fe_2(PO_4)_3$ *vs* $Fe_2(SO_4)_3$ and also to establish the relative energies of several redox couples, we chose to investigate the isostructural series of phosphates $Li_xMM'(PO_4)_3$ shown in Table I. The voltage plateaus were flat, representing two-phase regions, for $0 \ ^2\ x \ ^2\ 1$ in the parent compound. This behavior appears to reflect filling of the unique interstitial site per formula unit. Although there are three additional identifiable interstitial sites, it proved possible to intercalate reversibly more than four Li/formula unit; the $Li_{3+y}Fe_2(PO_4)_3$ system accepts $0 \ ^2\ y \ ^2\ 2$ additional Li atoms, for example, within a single solid-solution range. The voltage plateaus corresponding to a given redox energy were, in this structural family, essentially independent of the initial lithium concentration x.

TABLE I. Voltage plateaus at 0.05 mA/cm^2 for the phosphates $Li_xMM'(PO_4)_3$

x	MM'	Voltage Plateaus
0	TiNb	Ti^{4+}/Ti^{3+} = 2.5 V; Nb^{5+}/Nb^{4+} = 2.2 V; Nb^{4+}/Nb^{3+} = 1.7 V
1	Ti_2	Ti^{4+}/Ti^{3+} = 2.5 V
	FeNb	Fe^{3+}/Fe^{2+} = 2.8 V, Nb^{5+}/Nb^{4+} = 2.2 V, Nb^{4+}/Nb^{3+} = 1.7 V
2*	FeTi	Fe^{3+}/Fe^{2+} = 2.8 V, Ti^{4+}/Ti^{3+} = 2.5 V
3	Fe_2	Fe^{3+}/Fe^{2+} = 2.8 V
Li_2Na	V_2	V^{4+}/V^{3+} = 3.8V; V^{3+}/V^{2+} = 1.8V

* Solid solution with separate plateaus unresolved.

Stabilization of the vanadium compounds in the rhombohedral structure required the presence of at least one Na^+ ion, so the starting composition was $Li_2NaV_2(PO_4)_3$; lithium atoms were inserted to probe the V^{3+}/V^{2+} couple and extracted to obtain the energy of the V^{4+}/V^{3+} couple [14]. A separation of these two couples by 2 eV is compatible with the known chemistry of the vanadium oxides. The $Li_3Fe_2(PO_4)_3$ synthesized directly has the monoclinic structure pictured in Fig. 4; the rhombohedral form was obtained from $Na_3Fe_2(PO_4)_3$ by ion exchange in molten $LiNO_3$.

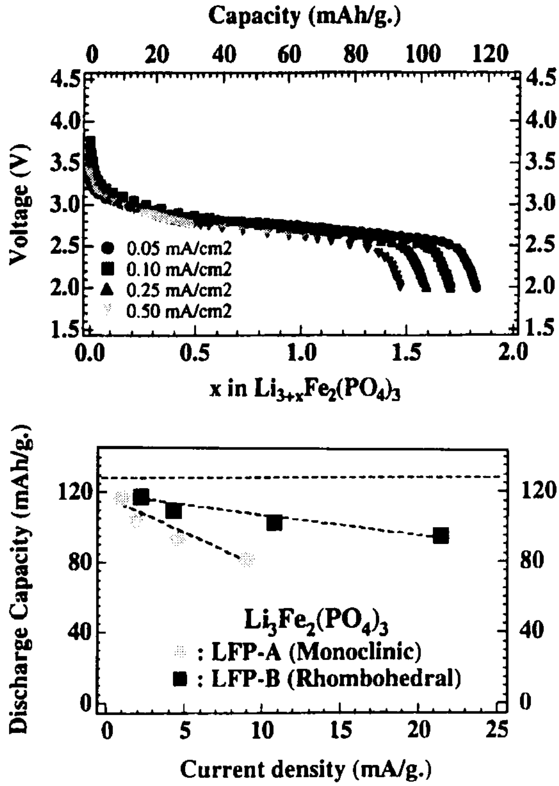

FIGURE 5 Cell voltages vs lithium for several current densities with rhombohedral $Li_{3+x}Fe_2(PO_4)_3$ cathode; comparison of the rate of capacity fade with increasing current density for the rhombohedral and monoclinic host structures.

Fig. 5 illustrates a reversible capacity fade that occurs with increasing current density; this type of capacity fade occurring with little loss in the V_{oc} of the solid-solution (or two-phase) plateau is greater the lower the mobility of the Li^+ ions, as is shown by the comparison in Fig. 5

of the rate of capacity fade in the monoclinic *vs* the rhombohedral forms of $Li_{3+y}Fe_2(PO_4)_3$. We interpret this capacity fade to be due to a decreasing area of the diffusion front that moves in from the surface of a particle to its core on lithium insertion. The current density that can be passed across the diffusion front becomes diffusion-limited at a critical area of the front, and the critical area is larger the lower is the Li^+-ion mobility.

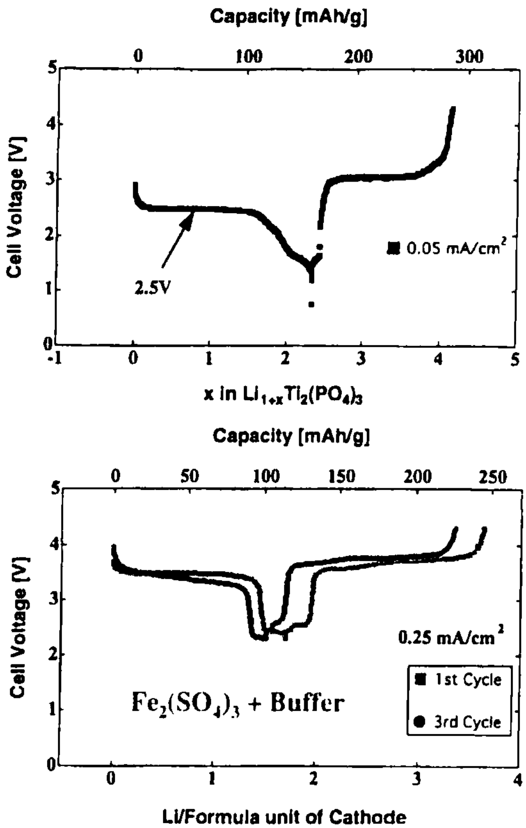

FIGURE 6 Cell voltage vs lithium of $Li_{1+x}Ti_2(PO_4)_3$ at 0.05 mA/cm^2 alone and as a buffer against overdischarge of $Li_xFe_2(SO_4$

Fig. 6 illustrates the use of a second phase of lower V_{oc} to act as a buffer against over-discharge. In this figure, $LiTi_2(PO_4)_3$ with a V_{oc} Å 2.5 V is acting as a buffer for $Fe_2(SO_4)_3$ with a V_{oc} Å3.6 V.

Fig. 7 illustrates the resolution of three plateaus in $Li_{1+y}FeNb(PO_4)_3$, the Fe^{3+}/Fe^{2+} couple at 2.8 V, Nb^{5+}/Nb^{4+} couple at 2.2 V, and the Nb^{4+}/Nb^{3+} couple at 1.7 V (current density = 0.05 mA/cm^2).

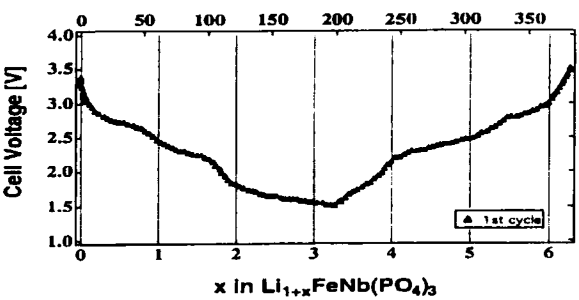

FIGURE 7 Resolution of three plateaus in the cell voltage vs. lithium at 0.05 mA/cm^2 of $Li_xFeNb(PO_4)_3$.

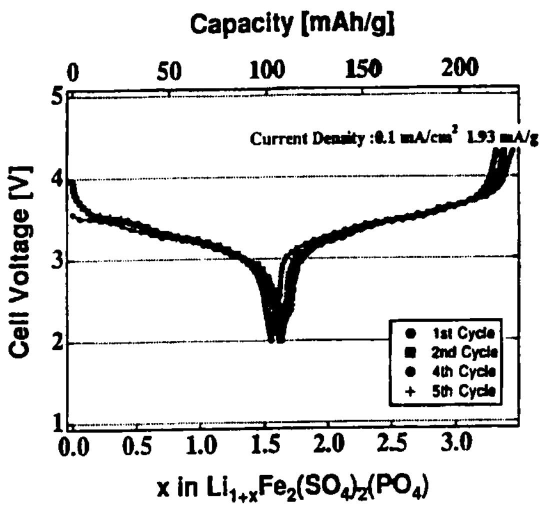

FIGURE 8 Cell voltage vs lithium at 0.05 mA/cm^2 of $Li_x(SO_4)_2(PO_4)$.

Fig. 8 illustrates the voltage *vs* lithium for $Li_{1+x}(SO_4)_2(PO_4)$ taken at 0.1 mA/cm^2 (1.93 mA/g) [14]. Since the Fe atoms are bridged by a mixture of $(SO_4)^{2-}$ and $(PO_4)^{3-}$ polyanions, the voltage lies between those for the sulfate and the phosphate without a double plateau.

CONCLUSIONS

The following conclusions may be drawn from this work:

- Lithium-insertion compounds allow determination of the redox energies of the transition-metal ions in the host matrix relative to the Fermi energy of a lithium anode.
- Where two transition-metal cations are present in a host matrix, they give separate voltage plateaus characteristic of a local equilibrium bond length.
- The **relative** energies of the several redox couples listed in table I remain fixed on going from one structure to another or from one polyainon to another in an isostructural family, but the **absolute** energies of all the couples changes.
- Candidate cathode materials for Li^+ - ion batteries have been identified that operate on environmentally benign Fe^{3+}/Fe^{2+}, Mn^{3+}/Mn^{2+}, or V^{4+}/V^{3+} couples.
- More open frameworks containing polyanions give **higher power capabilities** than hosts with close-packed oxide-ion arrays, the gain in Li^+-ion mobility more than offsetting the decrease in electronic conductivity; however, there is a loss in capacity per unit volume.
- A buffer against over-discharge or over-charge is a viable option.
- A reversible capacity fade at higher current density reflects the onset of the diffusion limit at a critical surface area of the diffusion front.

ACKNOWLEDGMENTS

The Robert A. Welch Foundation, Houston, TX, and the Institute for Advanced Technology (IAT) at the University of Texas at Austin, federated with the U.S. Army Research Laboratory, are thanked for financial support.

REFERENCES

[1.] A.C.W.P. James and J.B. Goodenough, Solid State Ionics **27**, 37(1988) and references therein.

[2.] M.S. Whittingham, Prog. Solid State Chem. **12**, 41 (1976)

[3.] M.G.S.R. Thomas, P.G. Bruce and J.B. Goodenough, Solid State Ionics, **17**, 13(1985).

[4.] J.B. Goodenough, M.M. Thackeray, W.I.F. David, and P.G. Bruce, Rev. Chim. Min. **21**, 435(1984)

[5.] J.B. Goodenough, A. Manthiram, and B. Wnetrzewski, *J. Power Sources* **43-44**, 269(1993).

[6.] M.M. Thackeray, P.J. Johnson, L.A. DePicciotto, P.G. Bruce and J. B. Goodenough, Mater. Res. Bull. **19**, 179(1984).

[7.] G.T.K. Fey, W.Li, and J.R. Dahn, J. Electrochem. Soc. **141**, 2279(1994)

[8.] K.S. Nanjundaswamy, A.K. Padhi, C. Masquelier, S. Okada, and J.B. Goodenough, *Proc. 37th Power Sources Conference*, Cherry Hill, New Jersey, June 17, 1996.

[9.] A.K. Padhi, K.S. Nanjundaswamy, and J. B. Goodenough, J. Electrochem. Soc. **144**, 1188(1997).

[10.] J.B. Goodenough, "General Concepts" in *Lithium Ion Batteries*, M.Wakihara, ed. (Kodansha Scientific Ltd.), Tokyo, 1997). Chap. 1.

[11.] A.K. Padhi, K.S. Nanjundaswamy, S. Okada, C. Masquelier and J.B. Goodenough, *J. Electrochem. Soc.* (in press).

[12.] C. Masquelier, A.K. Padhi, K.S. Nanjundaswamy, S. Okada and J.B.Goodenough, J. Solid State Chem. (in press).

[13.] A. Manthiram and J.B. Goodenough, J. Power Sources **26**, 403(1989).

[14.] A.K. Padhi, V. Manivannan, and J.B. Goodenough, unpublished.